SCIENCE & GLOBAL SECURITY
2022, VOL. 30, NO. 3, 117–130
https://doi.org/10.1080/08929882.2022.2145777

Routledge
Taylor & Francis Group

Computational Fluid Dynamics Analysis of the Infrared Emission From a Generic Hypersonic Glide Vehicle

Graham V. Candler[a] and Ivett A. Leyva[b]

[a]Aerospace Engineering & Mechanics, University of Minnesota, Minneapolis, MN, USA;
[b]Aerospace Engineering, Texas A&M University, College Station, TX, USA

ABSTRACT

Hypersonic boost-glide vehicles are designed to fly long distances in the upper atmosphere. They are reported to have the potential to evade ballistic missile early warning systems and to maneuver as they fly toward their target. A recent analysis by Tracy and Wright in *Science & Global Security* claimed to show that typical boost-glide vehicles produce significant infrared signatures that would be readily detectable with existing U.S. satellites and therefore questioned the potential advantages of hypersonic weapons over existing missiles. The prior analysis is revisited and several inconsistencies in the underlying assumptions are described. A detailed computational fluid dynamics analysis predicts typical infrared signatures to be significantly lower than those predicted by Tracy and Wright. As a result, these signatures would fall below the detection threshold of legacy U.S. Defense Support Program satellites but remain detectable by the more modern sensors from the Space-Based Infrared System. There are two significant issues with the prior analysis: an incorrect aerodynamic angle of attack was used, and the turbulent heat transfer rate correlation used to predict the surface temperature is inaccurate at the conditions studied.

ARTICLE HISTORY
Received 26 February 2022
Accepted 20 September 2022

Introduction

Recently, Cameron Tracy and David Wright published a paper in *Science & Global Security* that estimates the infrared (IR) emission from a generic hypersonic boost-glide vehicle (HGV).[1] They discuss the implications of their results for the detection of HGVs using existing ballistic missile early warning satellites. One of their main conclusions is that the IR emission from the glide vehicle surface would be detectable by the Defense Support Program (DSP) and the Space-Based Infrared System (SBIRS) satellites based on open-literature estimates of their sensor capabilities.

Tracy and Wright considered a hypersonic glide vehicle based on a geometry published by Niu et al.[2] They approximated the upper-facing

CONTACT Ivett A. Leyva ivett.leyva@tamu.edu Department of Aerospace Engineering, Texas A&M University, 710 Ross Street, Rm 710, College Station, TX 77843, USA.

surface that would be visible from a satellite as angled flat plates, and assumed that the heat transfer rate correlations of Tauber et al. are valid.[3] With these correlations and a radiative equilibrium boundary condition, in which the aerodynamic heating is balanced by re-radiative cooling, it is possible to estimate the surface temperature at a given flight condition. Tracy and Wright assumed a fully turbulent flow, and therefore the relevant Tauber et al. correlation ($V > 4\,\text{km/s}$) and the heat transfer rate balance are:

$$\left(\frac{dq}{dt}\right)_{FP} = 2.2 \times 10^{-5} \frac{(\cos\theta)^{2.08}(\sin\theta)^{1.6}}{x^{0.2}} \left(1 - \frac{1.11 h_w}{h_o}\right) \rho^{0.8} V^{3.7} \tag{1}$$

$$\left(\frac{dq}{dt}\right)_{rad} = \varepsilon\sigma T_w^4 = \left(\frac{dq}{dt}\right)_{FP} \tag{2}$$

where dq/dt is the heat transfer rate (W/m^2), θ is the angle of the flat plate surface relative to the freestream flow, ρ is the freestream density (kg/m^3), and V is the flight speed (m/s). The surface temperature is T_w (K) and h_w (J/kg) is the enthalpy of the gas at that temperature; h_o is the freestream total enthalpy (J/kg). For a fully turbulent flow, x (m) is the distance from the leading edge of the flat plate.[4] The second equation is the radiative equilibrium boundary condition, in which the re-radiation from the surface balances the aerodynamic heating assuming a gray body with emissivity ε. Tracy and Wright assume $\varepsilon = 0.85$ for a carbon heat shield material.

Tracy and Wright use these equations to estimate the surface temperature distribution on candidate boost-glide trajectories; these trajectories are computed assuming that the HGV is flying at its maximum lift-to-drag condition, which is assumed to be $L/D_{\max} = 2.6$. Then, using the Planck black body formula, they compute the infrared emission from the upward-facing surface for two bands in the short-wavelength IR.

In this paper, the Tracy and Wright analysis is examined to assess its validity and compare their results to predictions using computational fluid dynamics. The analysis presented here suggests that several assumptions made or retained by Tracy and Wright in their analysis are incorrect. As a result, they arrived at substantially larger values of IR emission than those obtained in the present work.

Computational fluid dynamics analysis

The University of Minnesota US3D computational fluid dynamics (CFD) code was applied to the problem studied by Tracy and Wright.[5] The code uses a finite volume method to numerically solve the governing equations of compressible fluid motion including viscous and high-enthalpy effects.[6]

For attached laminar flows, which as we show later are relevant here, the computed heat transfer rate predictions are usually within the error bars of experimental wind tunnel measurements, with typical errors of +/− 5%. Aerodynamic coefficients are typically predicted within experimental uncertainty, and prior work has shown excellent agreement between aerodynamic coefficient predictions and AEDC Tunnel 9 data for a waverider geometry (similar to the HGV studied here) at Mach 8 conditions.[7]

A computational grid of the representative HGV geometry was generated with the LINK3D software.[8] Figure 1 is a three-view of the modeled HGV based on the geometry taken from Niu et al. (also used by Tracy and Wright). The grid is clustered near the surface to resolve the large gradients in the boundary layer. The focus is on one of the conditions studied by Tracy and Wright: flight at 6 km/s and 49.7 km geopotential altitude (based on the U.S. Standard Atmosphere, the freestream density is $\rho = 1.015 \times 10^{-3}$ kg/m3 and temperature is $T = 270.65$ K).[9]

Due to the high-enthalpy flight conditions, the flow field is modeled with a 5-species reacting air chemical kinetics mechanism that represents nitrogen and oxygen dissociation and nitric oxide (NO) formation.[10] It is assumed that the surface is non-catalytic, meaning that the surface material does not promote gas-surface reactions that would cause recombination of reacted gas-phase species on the surface. At each finite volume face on the surface of the modeled HGV, the above radiative equilibrium boundary condition is applied with $\varepsilon = 0.85$; the aerodynamic heat transfer rate to the surface is a result of the computational solution as opposed to the Tauber et al. correlation.[11]

First, consider the aerodynamics of the generic HGV. The angle of attack, α, is varied from 0° to 20°, and the lift-to-drag ratio is computed. The angle of attack is measured in the coordinate system shown in Figure 1. Thus, the freestream velocity is given by

$$\vec{V} = V\cos\alpha\ \vec{i} + V\sin\alpha\ \vec{j} \tag{3}$$

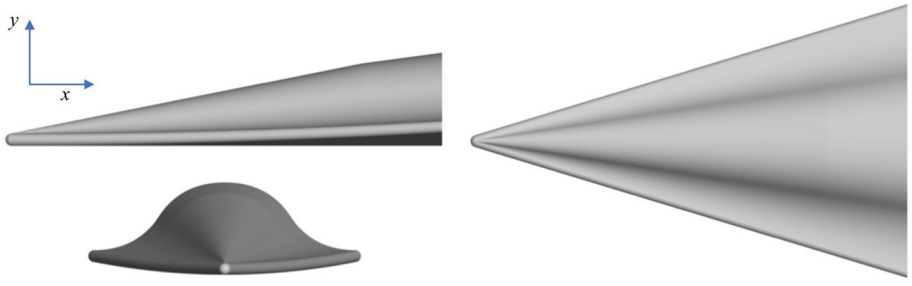

Figure 1. Three-view of the generic HGV geometry used in the present analysis modeled after Niu et al.

Laminar and turbulent CFD simulations were run; for the turbulent cases, the one-equation Spalart-Allmaras Reynolds-averaged Navier-Stokes model[12] was used. The predicted variation of L/D with angle of attack is plotted in Figure 2.[13] Note that for a laminar boundary layer, a maximum L/D of 2.58 is achieved at $\alpha = 14°$. The main effect of turbulence is to increase the drag due to surface shear stress, resulting in a lower L/D_{max} of 2.39 at $\alpha = 13°$.

Figure 3 plots the predicted upper and lower surface centerline temperature distributions for the laminar and turbulent CFD solutions at L/D_{max}. There is a significant difference in the lower surface temperature, but the difference is negligible on the upper surface. Thus, at the maximum L/D condition, the upper surface temperature distribution is not sensitive to the state of the boundary layer. For completeness, an approximate method for assessing boundary layer transition was used to evaluate whether the flow would be expected to be laminar or turbulent. The most widely used approach is to compute the ratio of the boundary layer momentum thickness Reynolds number, Re_θ, to the Mach number evaluated at the edge of the boundary layer, M_e. When this ratio exceeds a critical value (usually between 100 and 300), the boundary layer is susceptible to transitioning to turbulence.[14] The computed values of Re_θ/M_e are less than 100 on the upper surface, and reach just over 100 in a small region on the lower surface. Thus, even with the most conservative critical value, it is expected

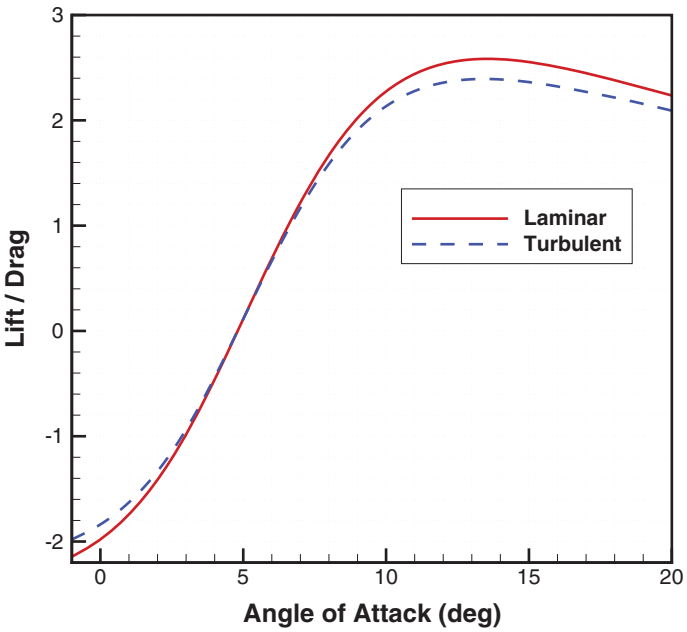

Figure 2. CFD prediction of the lift-to-drag ratio as a function of angle of attack of the generic HGV flying at 6 km/s and 49.7 km altitude.

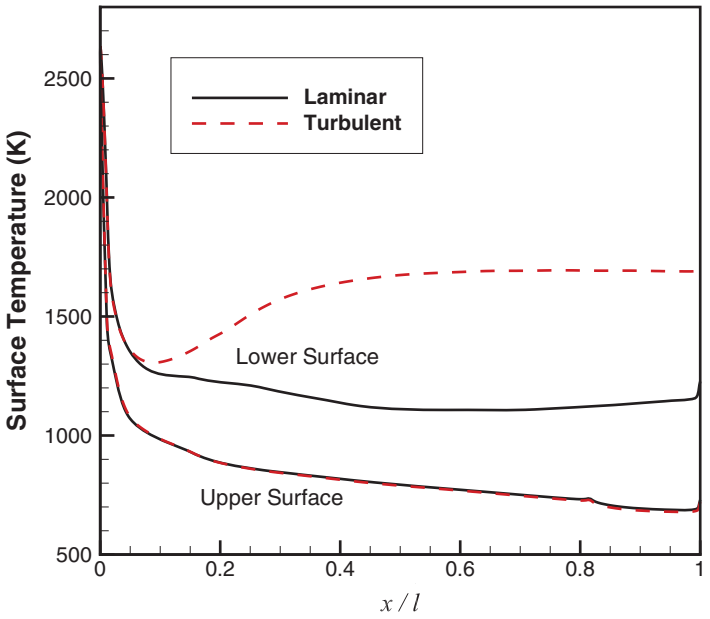

Figure 3. CFD predictions of the centerline temperature for the laminar and turbulent simulations at the angle of attack corresponding to maximum L/D. Flight condition: 6 km/s and 49.7 km altitude.

that the upper surface boundary layer will be fully laminar for this flight condition. More detailed analysis of complex three-dimensional boundary layer instability growth and transition to turbulence is becoming feasible with large-scale computation and advanced linear stability analysis methods.[15] However, this type of analysis is beyond the scope of the present work.

Based on the laminar CFD temperature distribution, Planck's law was integrated over the wavelength range of interest and over the HGV surface to obtain the upward-directed in-band IR emission, as in Tracy and Wright (their Equation 12). Figure 4 plots the variation of the predicted emission from the two short-wavelength IR bands considered by Tracy and Wright (2.69−2.95 μm and 1.4−3.0 μm) as a function of angle of attack.[16] As expected, the emission decreases as the upper surface is angled away from the freestream velocity vector; at the maximum L/D condition, the predicted emission from the narrow band is 4.90 kW/sr. This is significantly less than the value predicted by Tracy and Wright (43 kW/sr), and is well below the estimated sensitivity of the DSP (20 kW/sr) satellites. The emission from the wider SBIRS band is predicted to be 29.0 kW/sr, which is also significantly less than Tracy and Wright's estimate of approximately 370 kW/sr. However, the wide band emission is predicted to be above the estimated 6 kW/sr SBIRS detection threshold, making it likely that its

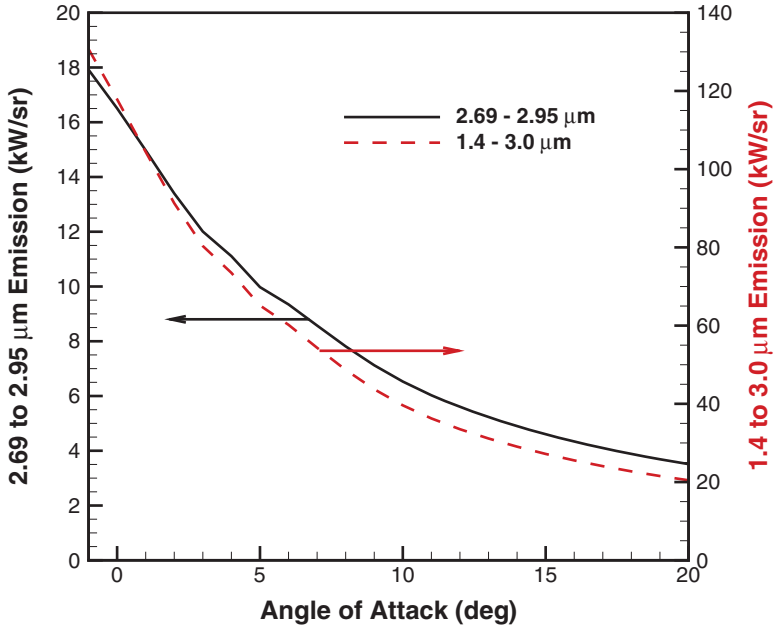

Figure 4. Predicted IR emission from the upper surface of the HGV as a function of angle of attack; two wavelength bands are plotted: DSP from 2.69 to 2.95 μm, and SBIRS from 1.4 to 3.0 μm. Flight condition: 6 km/s, 49.7 km altitude.

probability of detection would be sufficiently high with a potentially acceptable false alarm rate.[17]

The CFD simulations assumed a non-catalytic surface, in which the surface material is inert and there are no gas-surface reactions. However, this is not consistent with the assumption that the thermal protection system is composed of a carbon material, which may be ablating at the conditions considered. Therefore, a CFD case was run with a state-of-the-art finite-rate oxidation and nitridation ablation boundary condition to assess the effects of ablation on the IR hardbody signature.[18] Most of the ablation occurs on the leading edges of the HGV due to the high localized heat transfer rates and surface temperatures. The ablation boundary condition affects the energy balance at the surface, and in this case, it reduces the integrated heat transfer rate. Thus, the effect of ablation is to lower the IR emission by about 10% relative to the non-catalytic boundary condition.

There is another potential source of IR emission from the HGV: gas-phase emission from the high-temperature shock-layer and wake. The levels of this emission must be computed by solving a collisional-radiative model and the emission levels are highly dependent on the chemical species present in the flow field. The primary IR emitter from high-temperature air is nitric oxide (NO), and if ablation species are present, carbon monoxide and carbon dioxide may also emit in the IR. However, the gas-phase IR emission is typically much lower than the hardbody emission. For example,

Niu et al. study an HTV-2 type of vehicle at altitudes of between 30 and 70 km, and show that the spectral intensity of gas-phase IR emission is several orders of magnitude lower than the hardbody surface emission.[19]

Comparison with Tracy and Wright

As discussed above, there are large differences between the IR signatures predicted by CFD and the analysis of Tracy and Wright. In this section, the key reasons for this discrepancy are identified. Consider one of the results from Tracy and Wright: Figure 5 reproduces their upper surface centerline temperature distribution (Figure 10 from their paper) for the flight condition discussed above (6 km/s and 49.7 km altitude). Given this surface temperature distribution, the flow angle relative to the surface, θ, can be computed from Equations (1) and (2). The computed values of θ are plotted in Figure 5. For $x/l \lesssim 0.8$, $\theta = 5.8°$ and for $x/l \gtrsim 0.8$, $\theta = 3.9°$, where l is the overall vehicle length.

For the section $x/l \lesssim 0.8$, the upper surface of the modeled HGV has an angle of 11.3° in the reference frame (see the inset in Figure 5). Thus, Tracy

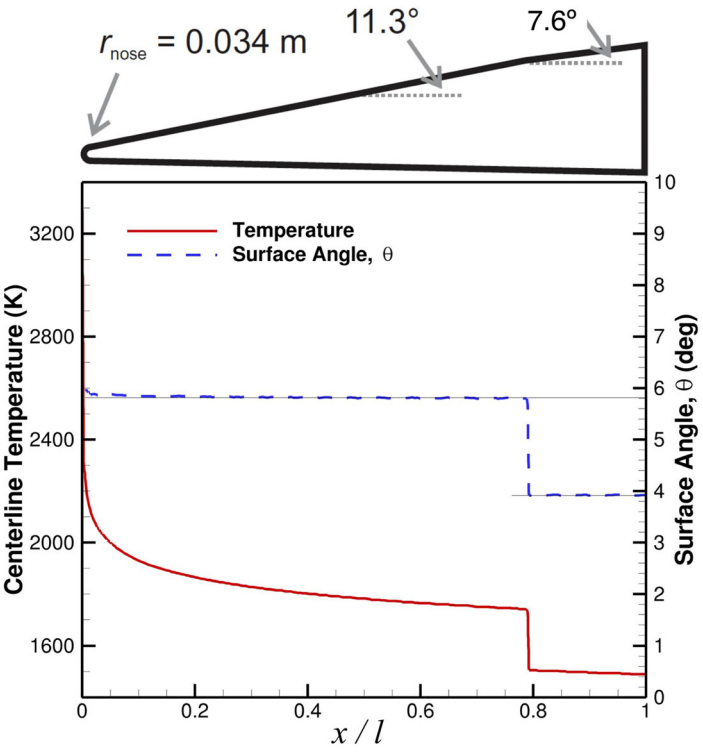

Figure 5. Solid line: upward-facing centerline surface temperature at flight conditions of 6 km/s and 49.7 km altitude taken from Tracy and Wright (Figure 10). Dashed line: surface angle relative to the freestream flow direction, θ, computed from Equations (1) and (2). The inset shows a side-view of the HGV geometry.

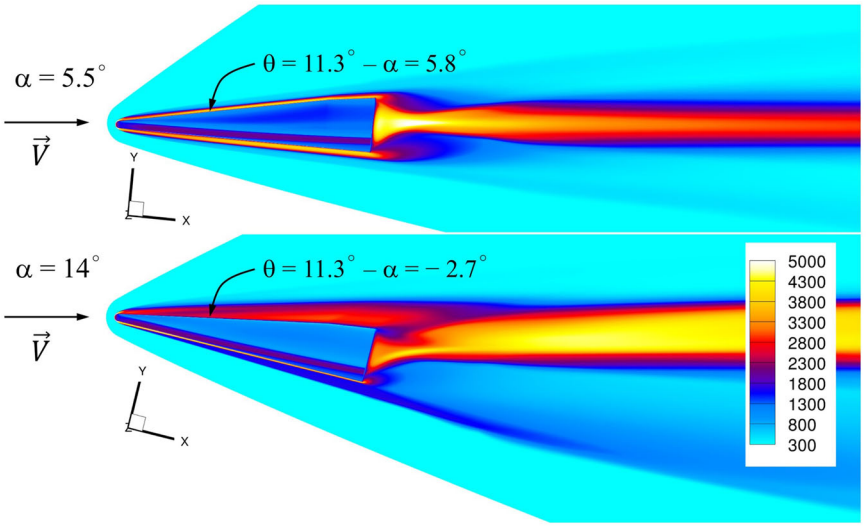

Figure 6. Visualization (temperature contours on the HGV surface and flow field symmetry plane) of the computed flow fields for the generic HGV. Top: $\alpha = 5.5°$, bottom: $\alpha = 14°$. Both images are oriented so that the freestream velocity is from left to right. The temperature scale was chosen to accentuate the flow features; the maximum value is close to 12,000 K in the nose region.

and Wright must have used an angle of attack of: $\alpha = 11.3° - \theta = 5.5°$. Figure 6 illustrates the difference in the HGV flight attitude for the angle of attack assumed by Tracy and Wright and for $\alpha = 14°$.

However, this angle of attack is not consistent with the assumed value of $L/D = 2.6$. See Figure 2: $\alpha = 5.5°$ gives $L/D = 0.40$. Figure 6 also illustrates that the flow directly impinges on the upper surface ($\theta > 0$) for $\alpha = 5.5°$, while for the $\alpha = 14°$ condition, $\theta < 0$. Furthermore, note that the heat transfer rate correlation, Equation (1), is not valid for $\theta < 0$ (produces an imaginary number).

Therefore, Tracy and Wright's assumed L/D is not consistent with their orientation of the model HGV relative to the freestream flow direction. Furthermore, the HGV would not be in stable flight at their implied angle of attack and corresponding L/D. This can be seen by considering the balance of forces in the flight-path normal direction. For equilibrium glide, the aerodynamic lift must balance gravity, less the centrifugal relief due to the curvature of the flight path:

$$\frac{L}{m} = g - \frac{V^2}{R} = \frac{1}{2}\rho V^2 \frac{1}{\beta}\frac{L}{D} \tag{4}$$

where R is the radius of curvature of the flight path, which is the radius of the Earth plus the flight altitude, and β is the ballistic coefficient, which Tracy and Wright assumed to be 13,000 kg/m^2. Substituting into this

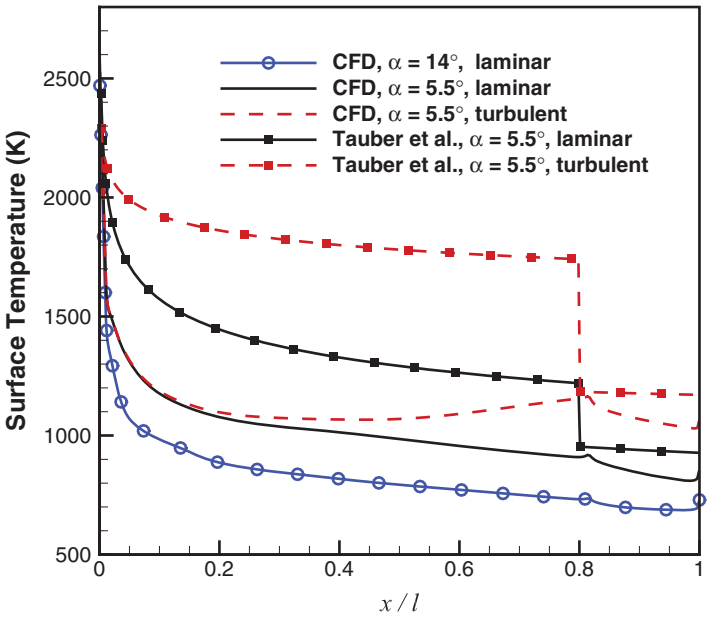

Figure 7. Upper centerline laminar and turbulent surface temperature distributions for $\alpha = 5.5^\circ$ predicted with CFD and the Tauber et al. correlation. Also plotted for reference is the $\alpha = 14^\circ$ laminar result.

equation shows that it is not satisfied for $L/D = 0.40$, and their HGV is not in stable level flight.

This inconsistency in the angle of attack explains part of the difference in the comparison with CFD. In addition, the Tauber et al. heat transfer rate correlation (Equation 1) is not accurate for the present conditions. Figure 7 compares the centerline surface temperature distribution computed with CFD and the correlation at $\alpha = 5.5^\circ$ for laminar and turbulent boundary layers; the laminar CFD result at $\alpha = 14^\circ$ is also plotted for reference. This shows that the Tauber et al. correlations significantly over-predict the surface temperature for these conditions. However, the Tauber et al. paper uses only two Space Shuttle Orbiter cases to establish the turbulent correlation (there is a third case, but it does not have a fully turbulent boundary layer). Furthermore, the correlation is applied at significantly different conditions than considered in the present work.[20] It should be noted that the U.S.3D CFD code has been compared to laminar and turbulent Shuttle Orbiter flight data for surface temperatures.[21] For almost all of the 16 thermocouples compared, the CFD predictions are within 100 K of the flight data. Thus, the difference in the predicted signatures is also due to the use of this inaccurate correlation.[22]

Tauber et al. make a conservative assumption that the surface is fully catalytic, which means that any reacted gas species that interact with the surface recombine due to gas-surface reactions catalyzed by the surface.

The CFD was rerun with a fully catalytic boundary condition, and it was found that the IR emission is increased by at most 6.9%.

Role of ballistic coefficient

There is an additional inconsistency in the assumptions made by Tracy and Wright that has an effect on the IR emission. They assume that the mass, m, of the HGV is 1000 kg, and as noted above, $\beta = m/(C_D A) = 13{,}000\,\mathrm{kg/m^2}$; C_D is the drag coefficient and A is the drag reference area. Drag is related to $C_D A$ with:

$$D = \frac{1}{2}\rho V^2 C_D A \tag{5}$$

The laminar CFD predicts the drag to be 3900 N at $\alpha = 14^\circ$. Thus, from the definition of β, we have $\beta = \frac{1}{2}\rho V^2 m/D = 4680\,\mathrm{kg/m^2}$, and the assumed ballistic coefficient is not consistent with level flight at the conditions assumed.

Substituting this corrected value of ballistic coefficient into Equation (4) yields a freestream density of 4.17×10^{-4} kg/m^3 at a flight speed of 6 km/s. The corresponding geopotential altitude is approximately 57.1 km based on the U.S. Standard Atmosphere. This assumes that the aerodynamic performance (C_D and L/D) does not change significantly at this higher altitude condition. When the CFD is rerun at this condition, the IR emission in the 2.69−2.95 μm band decreases to 2.95 kW/sr and in the 1.4−3.0 μm band to 22.1 kW/sr. Furthermore, this lower density condition reduces the likelihood of boundary layer transition, with the maximum value of $Re_\theta/M_e = 67$ on the upper surface.

Effect of freestream conditions on IR signature

The prior analysis focused on a 6 km/s flight speed. Now consider how variations in flight speed affect the IR emission from the generic HGV. As discussed above, the flight conditions cannot be chosen arbitrarily: for a given ballistic coefficient, L/D, and flight speed, there is a unique altitude where the HGV is in equilibrium glide. For this analysis, $\beta = 4{,}680$ kg/m^2 and $L/D = 2.6$ are held fixed, and the flight speed is varied from 3 km/s to 7 km/s. Figure 8 plots the upper surface emission in the two bands considered; note that for $3 \leq V \leq 6$ km/s the variation of IR emission is approximately linear with speed. This linear scaling occurs because the freestream density decreases with velocity squared, as can be seen by rearranging the glide condition

$$\rho = \frac{2\beta}{L/D}\left(\frac{g}{V^2} - \frac{1}{R}\right) \tag{5}$$

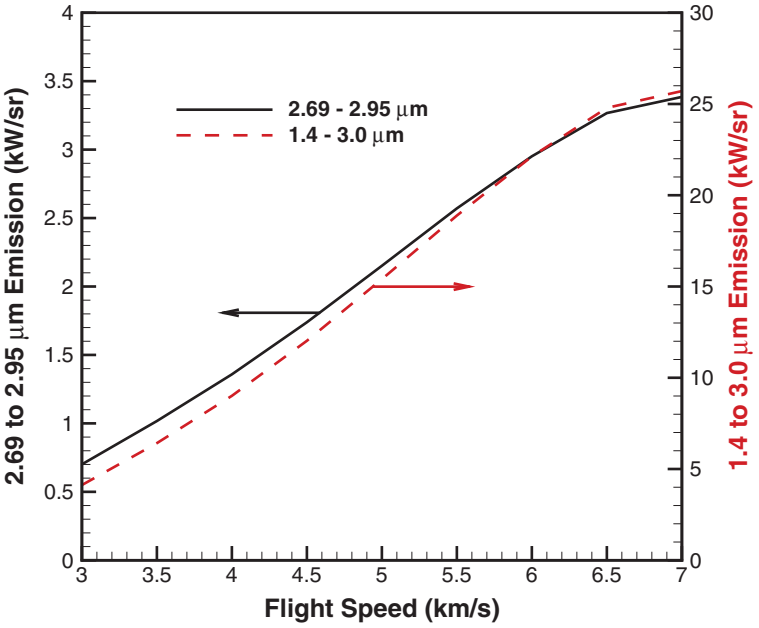

Figure 8. Predicted IR emission from the upper surface of the HGV as a function of flight speed at equilibrium glide conditions with $\beta = 4680$ kg/m^2 and $L/D = 2.6$.

Then, since the heat transfer rate is expected to scale roughly with $dq/dt \sim \rho V^3$, linear scaling with flight speed is obtained for $g/V^2 \gg 1/R$. From this relationship, it is also clear that HGVs with a larger ballistic coefficient and/or lower L/D will fly at a higher density (lower altitude), with a correspondingly larger surface temperature and IR signature.

Summary and conclusions

The computational fluid dynamics analysis presented here exposes several inconsistencies in the assumptions made by Tracy and Wright. It is shown that Tracy and Wright assumed a flight condition corresponding to an angle of attack of 5.5°, however, this is not consistent with the assumed lift-to-drag ratio of the HGV. The CFD analysis shows that the maximum lift-to-drag ratio of the generic HGV occurs at 14° angle of attack, and this flight condition significantly lowers the heat transfer rate to the upper surface. In addition, Tracy and Wright assume that the boundary layer is fully turbulent, which is not consistent with the low Reynolds number, high-altitude conditions associated with HGV equilibrium glide. Furthermore, the CFD analysis shows that a turbulent boundary layer would not significantly affect the upper surface temperature at the L/D_{max} condition. Using the correct angle of attack reduces the predicted upper surface temperature. Furthermore, the heat transfer rate correlation used by Tracy and Wright

significantly over-predicts the level of aerodynamic heating at the conditions studied. The combination of these errors results in an over-prediction of the upper surface temperature.

Additionally, the assumed ballistic coefficient of $\beta = 13,000$ kg/m^2 is not consistent with the aerodynamics of the generic HGV. Instead, for the assumed mass of 1000 kg, β should be significantly smaller based on the aerodynamic drag predicted by the CFD. This lower value of β results in a higher altitude glide condition and an even lower IR emission.

The current computational fluid dynamics analysis predicts that the generic HGV flying at its maximum lift-to-drag ratio and 6 km/s would produce short-wavelength IR signatures that are significantly lower than those predicted by Tracy and Wright (for the 2.65−2.95 μm band, 2.95 kW/sr vs. 43 kW/sr; for the 1.4−3.0 μm band, 22.1 kW/sr vs. 370 kW/sr). These signatures would be expected to be below the DSP detection threshold, but would still be detectable by SBIRS. These results assume a laminar boundary layer with a non-catalytic surface in radiative equilibrium. It is found that at the condition studied, the upward-directed IR emission is marginally sensitive to the effects of surface catalysis, ablation, and turbulence in the boundary layer; these effects change the predicted emission levels by less than 10%.

Tracy and Wright claim that there are social origins ("heterogeneous engineering") to the purported misperceptions about the capabilities of hypersonic weapons, including the perceived difficulty of detecting them during flight. However, the present analysis shows that this claim is not correct, and a fully consistent analysis is required to accurately characterize the performance and signatures of hypersonic weapons. The present work is based on computational fluid dynamics methods and computer code developed under basic research funding from the Department of Defense. The underlying numerical algorithms and physics models are published in the open literature and have been subjected to peer review. The work presented has not been influenced by DoD officials, is not subjective, and can be replicated by others.

Notes and References

1. C. L. Tracy and D. Wright, "Modeling the Performance of Hypersonic Boost-Glide Missiles," *Science & Global Security* 28, no. 3 (2020): 135–170.
2. Q. Niu, Z. Yuan, B. Chen, and S. Dong, "Infrared Radiation Characteristics of a Hypersonic Vehicle under Time-Varying Angles of Attack," *Chinese Journal of Aeronautics* 32, no. 4 (2019): 861–874.
3. M. E. Tauber, G. P. Menees, and H. G. Adelman, "Aerothermodynamics of Transatmospheric Vehicles," *Journal of Aircraft* 24, (1987) 594–602. See also, J. D. Anderson, *Hypersonic and High Temperature Gas Dynamics*, 2nd ed. (Reston, VA: AIAA, 2006), 349–50.

4. The Tauber et al. correlations are usually employed in two steps: first the laminar correlation is used from the leading edge to the transition location with x measured from the leading edge of the flat plate, and then the turbulent correlation is used with x measured from the transition location. A transition length is assumed between laminar and turbulent flow. See the discussion associated with Figure 2b in Tauber et al., 1987. Tracy and Wright assumed fully turbulent flow with transition occurring at the leading edge of the plate, and thus they measure x from the leading edge.
5. G. V. Candler, H. B. Johnson, I. Nompelis, V. M. Gidzak, P. K. Subbareddy, and M. B. Barnhardt, "Development of the US3D Code for Advanced Compressible and Reacting Flow Simulations," AIAA Paper 2015-1893, 53rd AIAA Aerospace Sciences Meeting, 5-9 January 2015, Kissimmee, Florida.
6. G. V. Candler, P. K. Subbareddy, and J. M. Brock, "Advances in Computational Fluid Dynamics Methods for Hypersonic Flows," *Journal of Spacecraft and Rockets* 52, no. 1 (2015): 17–28.
7. T. W. Drayna, I. Nompelis, and G. V. Candler, "Numerical Simulation of the AEDC Waverider at Mach 8," AIAA Paper 2006-2816, 25th AIAA Aerodynamic Measurement Technology and Ground Testing Conference, 05 June 2006 - 08 June 2006, San Francisco, California.
8. https://www.link-3d.com. The grid is composed on 15.4 million hexahedral elements and the simulations were run for over 100 body flow-through times and a reduction in solution residual of at least six orders of magnitude. The value of y^+ for the first grid point away from the surface is approximately 0.1 on the leading edges, and is well below unity on all surfaces. Generally, second-order accurate CFD simulations require $y^+ < 1$ for the computational grid to resolve the gradients at the surface and to produce an accurate prediction of the heat transfer rate; see https://www.cfd-online.com/Wiki/Dimensionless_wall_distance_(y_plus). The boundary layer is resolved with approximately 45 grid elements in the surface-normal direction. These grid properties are more than sufficient to obtain accurate aerodynamic forces and heat fluxes, such as in the CFD results reported in AIAA 2006-2816.
9. US Standard Atmosphere, 1976, NASA Technical Memorandum TM-X-74335, 1976. Also https://www.digitaldutch.com/atmoscalc/
10. C. Park, "Review of Chemical-Kinetic Problems of Future NASA Missions. I – Earth Entries," *Journal of Thermophysics and Heat Transfer* 7, no. 3 (1993): 385–398.
11. The radiative equilibrium boundary condition ignores conduction into and out of the vehicle; thus, it will tend to over-predict the surface temperature early in the trajectory when the vehicle is cold.
12. P. R. Spalart and S. R. Allmaras, "A One-Equation Turbulence Model for Aerodynamic Flows," *Recherche Aerospatiale* 1 (1994): 5–21. See also the "Standard" Spalart-Allmaras One-Equation Model at https://turbmodels.larc.nasa.gov/spalart.html
13. By definition, drag is the component of the aerodynamic force opposed to the motion of the flight vehicle, and lift is the component of aerodynamic force perpendicular to the direction of motion.
14. J. D. Anderson, *Hypersonic and High-Temperature Gas Dynamics*, 2nd ed. (Reston, VA: AIAA, 2006), 335; S. Berry, K. Daryabeigi, K. Wurster, and R. Bittner, "Boundary Layer Transition on X43-A," *Journal of Spacecraft and Rockets* 47, no. 6 (2010): 922–34.
15. X. Chen, S. Dong, G. Tu, X. Yuan, and J. Chen, "Boundary Layer Transition and Linear Modal Instabilities of Hypersonic Flow Over a Lifting Body," *Journal of Fluid Mechanics,* 938 (2022): A8; see also, for example: D. B. Araya, N. P. Bitter, B. M.

Wheaton, O. Kamal, T. Colonius, A. Knutson, H. Johnson, J. Nichols, G. V. Candler, V. Russo, et al., "Assessment of Linear Methods for Analysis of Boundary-Layer Instabilities on a Finned Cone at Mach 6," AIAA Aviation 2022 Forum, June 27–July 1, 2022 Chicago, IL.

16. As the angle of attack increases, the flow is less directed toward the surface, and it would appear that the flow should detach or separate from the upper surface at a critical angle of attack. However, at hypersonic conditions flow separation does not occur until angles of attack greater than considered here; rather, the flow remains attached and expands around the leading edge. This accounts for the smooth variation of the IR emission with angle of attack.
17. D. K. Barton, Roger Falcone, Daniel Kleppner, Frederick K. Lamb, Ming K. Lau, Harvey L. Lynch, David Moncton, David Montague, David E. Mosher, William Priedhorsky, et al., "Report of the American Physical Society Study Group on Boost-Phase Intercept Systems for National Missile Defense: Scientific and Technical Issues," *Reviews of Modern Physics*, 76, no. 3 (2004): S167–168.
18. K. S. Prata, T. E. Schwartzentruber, and T. K. Minton, "Air-Carbon Ablation Model for Hypersonic Flight from Molecular-Beam Data," *AIAA Journal*, 60, no. 2 (2022): 627–40.
19. Q. Niu, S. Yang, Z. He, and S. Dong, "Numerical Study of Infrared Radiation Characteristics of a Boost-Gliding Aircraft with Reaction Control Systems," *Infrared Physics & Technology*, 92 (2018): 417–28.
20. Tauber et al. Case 1: 2640 m/s, $Re_L = 7.6 \times 10^6$, $a = 34.1°$; Case 2: 2275 m/s, $Re_L = 10.6 \times 10^6$, $a = 30.8°$, where Re_L is the Reynolds number based on freestream conditions and vehicle length. The present case has $Re_L = 1.3 \times 10^6$.
21. G. V. Candler and C. H. Campbell, "Hypersonic Navier-Stokes Comparisons to Orbiter Flight Data," AIAA Paper No. 2010-0455 (2010), 48th AIAA Aerospace Sciences Meeting Including the New Horizons Forum and Aerospace Exposition, 04 January 2010 - 07 January 2010, Orlando, Florida.
22. There is an additional issue here. As discussed in Endnote 4, the laminar correlation should be used prior to transition, and then the turbulent correlation is used with x measured from the transition location. Tracy and Wright assume turbulent flow from the leading edge and as a result drastically over-estimate the surface temperature.